

# Itaconic Acid Is a Mammalian Metabolite Induced during Macrophage Activation

Cheryl L. Strelko,<sup>†</sup> Wenyun Lu,<sup>#</sup> Fay J. Dufort,<sup>§</sup> Thomas N. Seyfried,<sup>§</sup> Thomas C. Chiles,<sup>§</sup> Joshua D. Rabinowitz,<sup>#</sup> and Mary F. Roberts<sup>\*,†</sup>

Departments of <sup>†</sup>Chemistry and <sup>§</sup>Biology, Boston College, Chestnut Hill, Massachusetts 02467, United States

<sup>#</sup>Lewis-Sigler Institute for Integrative Genomics and Department of Chemistry, Princeton University, Princeton, New Jersey 08544, United States

**S** Supporting Information

**ABSTRACT:** Itaconic acid (ITA), or methylenesuccinic acid, is not generally classified as a mammalian metabolite. Using NMR-based metabolomics and <sup>13</sup>C-labeling, we have detected ITA in both macrophage-like VM-M3 and RAW 264.7 tumor cell lines as well as stimulated and unstimulated primary murine macrophages. Macrophage activation by addition of lipopolysaccharide and IFN- $\gamma$  markedly increased ITA production and secretion. Crude cell extracts synthesize ITA via decarboxylation of *cis*-aconitate, indicative of a novel mammalian *cis*-aconitic decarboxylase activity. Our results highlight a previously unidentified biosynthetic pathway related to TCA cycle metabolism in mammalian cells and a novel metabolite that likely plays a role in macrophage-based immune response.

Small-molecule effectors of cells are often overlooked. A case in point is itaconic acid (ITA), or methylenesuccinic acid, a metabolite made and secreted by the fungal organism *Aspergillus terreus*.<sup>1,2</sup> The biosynthesis of this dicarboxylic acid has been of interest because it can be used as a starting material for chemical synthesis of polymers.<sup>3,4</sup> More recently, ITA has been identified in a small number of cases of metabolomic analysis of mammalian tissue specimens.<sup>5–7</sup> In those few cases, whether it was synthesized by mammalian cells or endogenous flora, or arose merely as an adventitious contaminant, was unknown. Despite the overall lack of study of ITA as a mammalian metabolite, there is evidence that ITA can be catabolized by both guinea pig and rat liver mitochondria.<sup>8,9</sup>

The VM-M3 murine tumor cell line is derived from a spontaneously arising brain tumor in a VM mouse.<sup>10</sup> This cell line, reported to be metastatic, is similar in morphology to the well-characterized RAW 264.7 murine macrophage cell line, and both share properties of macrophages including gene expression and phagocytic capability.<sup>11,12</sup> We detected ITA in 1D-gHSQC NMR experiments (obtained on a Varian 600 MHz VNMRs equipped with a triple-resonance probe) with methanol/water (80:20) extracts of VM-M3 cells that had been incubated with [<sup>13</sup>C<sub>5</sub>]-glutamine or [<sup>13</sup>C<sub>6</sub>]-glucose. [<sup>13</sup>C<sub>5</sub>]-Glutamine resulted in detection of proton resonances at 3.15 ppm characteristic of the ITA signal for the <sup>-13</sup>CH<sub>2</sub>- moiety; [<sup>13</sup>C<sub>6</sub>]-glucose incubation gave rise to resonances consistent with labeled <sup>-13</sup>CH<sub>2</sub>- and =<sup>13</sup>CH<sub>2</sub> (at 5.37 and 5.85 ppm) groups.<sup>13</sup> The <sup>13</sup>C-labeled

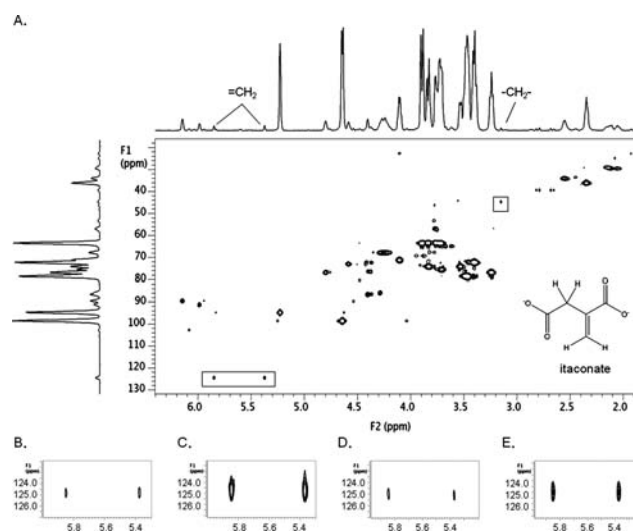


**Figure 1.** (A) 2D-gHSQC spectrum of methanol extracts of VM-M3 cells ( $8 \times 10^6$  cells) incubated with 25 mM [<sup>13</sup>C<sub>6</sub>]-glucose for 12 h. Inset: structure of itaconate. Slices from 2D-gHSQC spectra diagnostic for ITA are shown for extracts of RAW 264.7 cells ( $10^7$  cells) that were (B) unstimulated or (C) stimulated with 10 ng/mL LPS for 24 h, and extracts from murine macrophages ( $8 \times 10^6$  cells) that were (D) unstimulated or (E) stimulated by priming with 150 U/mL IFN- $\gamma$  for 6 h followed by 24 h incubation with 10 ng/mL LPS prior to incubation with 25 mM [<sup>13</sup>C<sub>6</sub>]-glucose for 12 h. For spectra A–C, nt = 128 and ni = 128. For spectra D and E, nt = 256 and ni = 128.

ITA was present at sufficiently high levels that it could easily be identified using 2D-gHSQC (Figure 1A) and 2D-gHSQC-TOCSY experiments. The <sup>1</sup>H resonances arising from itaconate were also confirmed by doping cell extracts with an itaconate standard. Using the size of the VM-M3 cells and cell count used for the extracts, and quantifying the amount of ITA in the extracts using MS methods, we estimate the intracellular concentration of this compound to be  $1.33 \pm 0.16$  mM.

<sup>13</sup>C-Labeled ITA was also detected by 1D-gHSQC in an extract of the culture medium (Figure 2) in which cells were incubated with [<sup>13</sup>C<sub>6</sub>]-glucose for 12 h. In order to detect the ITA, the large amount of [<sup>13</sup>C<sub>6</sub>]-glucose was removed from the resolubilized extract with Strata-X-A solid-phase extraction

Received: August 6, 2011

Published: September 15, 2011

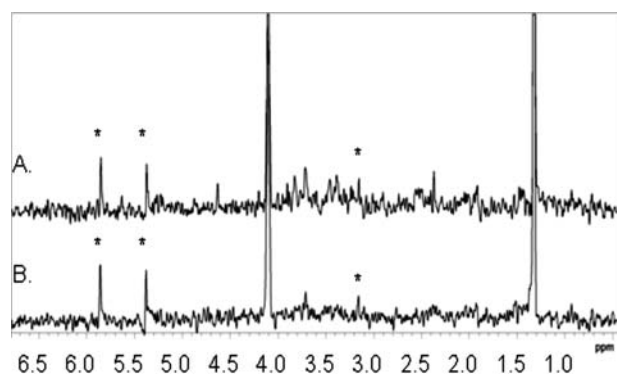


**Figure 2.** 1D-gHSQC spectra of culture media from (A) RAW 264.7 cell cultures stimulated with 10 ng/mL LPS and (B) VM-M3 cell cultures that were incubated with [ $^{13}\text{C}$ ]glucose for 12 h and then treated to isolate weak acids including ITA (\*). 6400 transients were collected for each spectrum.

cartridges (see Supporting Information (SI) for detailed treatment). Thus, this molecule appears to be secreted by the cells.

ITA may be a metabolite associated with a wide variety of tumors, or it could occur in a unique subset. We therefore investigated ITA synthesis in the macrophage-like RAW 264.7 cell line and the unrelated MCF-7 breast cancer cell line. Although  $^1\text{H}$  NMR has been used to profile the RAW 264.7 metabolome,<sup>14,15</sup> the relatively low concentration of ITA would make it difficult to detect in the absence of  $^{13}\text{C}$ -labeling and selective analysis of protons coupled to  $^{13}\text{C}$ . gHSQC spectra of extracts from unstimulated RAW 264.7 cells incubated with [ $^{13}\text{C}_6$ ]glucose exhibited a detectable amount of ITA (Figure 1B), while extracts from the MCF-7 cell line incubated with the labeled glucose did not contain NMR-detectable levels of ITA. Moreover, analysis of several unrelated cell types (*Escherichia coli* strain NCM3722, *Clostridium acetobutylicum* strain ATCC 824, *Saccharomyces cerevisiae* strain CEN-PK, cultured human foreskin fibroblasts, or pancreatic tumor tissue) by LC-MS failed to reveal detectable levels of ITA. It is noteworthy that stimulation of RAW 264.7 cells with lipopolysaccharide (LPS) resulted in an increased level of detectable  $^{13}\text{C}$ -ITA (Figure 1C); ITA was also detected in the tissue culture media of the RAW 264.7 cells as well as VM-M3 cells (Figure 2). Thus, ITA synthesis is not a generic characteristic of all tumor cell lines, and might instead be indicative of those of macrophage lineage.

To test the possibility that ITA synthesis is a characteristic of macrophages, we analyzed unstimulated mouse peritoneal macrophages and activated macrophages following *ex vivo* stimulation with IFN- $\gamma$  and LPS that were then incubated with [ $^{13}\text{C}_6$ ]glucose. While very low levels of ITA could be detected in the unstimulated cell extracts (Figure 1D), a dramatic increase was observed in the activated cells (Figure 1E). This is consistent with the findings of Shin et al.,<sup>5</sup> who detected ITA in the lungs of mice infected with *Mycobacterium tuberculosis*, the primary site of inflammation and macrophage response to infection, but not other organs. As with the VM-M3 cells, ITA was also detected in the culture medium, but only in cells that had been stimulated with LPS. Therefore, production of ITA may represent a previously unrecognized facet of the macrophage-mediated immune response.

Multiple pathways have been proposed for the biosynthesis of ITA<sup>1,16,17</sup> (SI, Figure S2). To distinguish among these, we used isotope tracers. The low concentration of ITA in the  $^{13}\text{C}$ -labeled

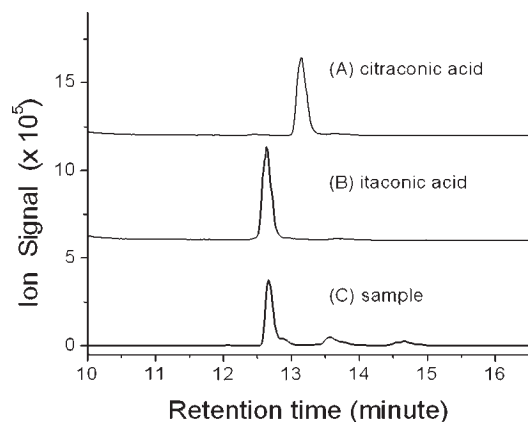


**Figure 3.** Representative chromatographic traces for the detection of itaconic acid. (A) Standard of citraconic acid (5  $\mu\text{g}/\text{mL}$ ), a structural isomer of ITA, with a retention time of 13.2 min and detected mass of 129.0196 (error of 2.3 ppm) compared to the theoretical mass of 129.0193, in negative ion mode. (B) Standard of ITA (5  $\mu\text{g}/\text{mL}$ ), with a retention time of 12.70 min and detected mass of 129.0195 (1.5 ppm error). (C) ITA detected in the cellular extract of VM-M3 cell line, with a detected mass of 129.0195 (1.5 ppm error).

extracts made direct  $^{13}\text{C}$  detection by NMR impractical. Therefore, we used LC-MS measurements<sup>18</sup> of ITA and its potential precursors, including acetyl CoA, pyruvate, citrate, and aconitate, after incubating cells with [ $^{13}\text{C}_6$ ]glucose or [ $^{13}\text{C}_5$ ]glutamine (Figure 3).

If the biosynthesis of ITA in mammalian cells occurs through the same pathway as in *Aspergillus* (decarboxylation of *cis*-aconitate followed by a 1,3-allylic rearrangement catalyzed by *cis*-aconitic decarboxylase, Figure 4A),<sup>1,19,20</sup> then incubation of the cells with [ $^{13}\text{C}_5$ ]glutamine should yield [ $^{13}\text{C}_4$ ]ITA as the primary isotopologue from the first turn of the TCA cycle. This results from glutamine hydrolysis to glutamate followed by transamination and production of  $\alpha$ -ketoglutarate, which then enters the TCA cycle. This would ultimately result in [ $^{13}\text{C}_4$ ] *cis*-aconitate that is site-specifically decarboxylated to [ $^{13}\text{C}_4$ ]ITA (Figure 4B). [ $^{13}\text{C}_4$ ]ITA is indeed the major isotopologue of itaconic acid present under these conditions (see SI, Figure S4). This pathway is further supported by the fact that we see vastly more  $^{13}\text{C}$ -label at the  $-\text{CH}_2-$  position than the  $=\text{CH}_2$  position by 1D-gHSQC NMR. Incubation of cells with [ $^{13}\text{C}_6$ ]glucose, with the same biosynthetic scheme, should generate [ $^{13}\text{C}_1$ ]ITA resulting from the [ $^{13}\text{C}_2$ ]acetyl CoA that enters the TCA cycle and is converted to *cis*-aconitate, with one of the labeled carbons site-specifically lost during the *cis*-aconitate decarboxylase reaction (Figure 4C). This  $^{13}\text{C}$  flux through pyruvate dehydrogenase (PDH) does indeed result in the major isotopologues observed by MS, although there is also appreciable flux through pyruvate carboxylase (PC).<sup>21,22</sup> PC generates [ $^{13}\text{C}_3$ ]oxaloacetate that will ultimately result in the [ $^{13}\text{C}_4$ ]ITA isotopologues (Figure 4D). By comparing the percentage of total isotopologues of ITA resulting from PDH and PDH+PC flux ([ $^{13}\text{C}_1$ ] and [ $^{13}\text{C}_4$ ], respectively) to the percentage of total isotopologues of anticipated precursors citrate and aconitate from both PDH and PDH+PC fluxes ([ $^{13}\text{C}_2$ ] and [ $^{13}\text{C}_5$ ], respectively), we see that the three metabolites show comparable percentages from each flux. The isotope labeling data we have obtained (Figure 4E) are thus fully consistent with a biosynthetic pathway in mammalian cells whereby ITA is synthesized via the specific decarboxylation of *cis*-aconitate from

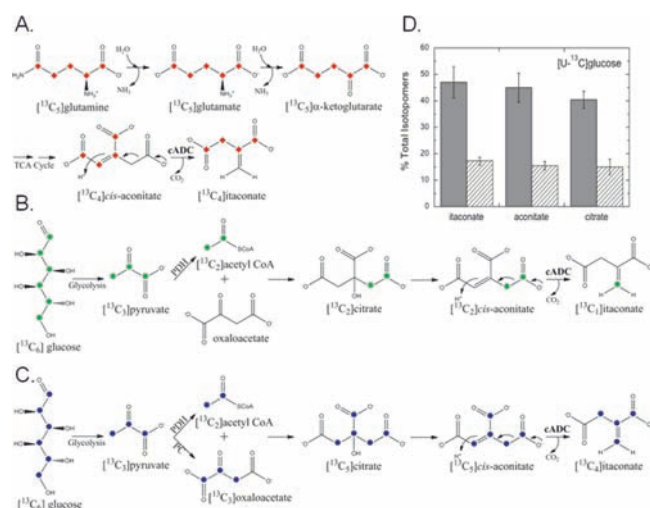


**Figure 4.** ITA labeling schemes and isotopologues distribution in itaconate, aconitate, and citrate for the first turn of the TCA cycle in VM-M3 cells incubated for 12 h with [U-<sup>13</sup>C]glutamine or [U-<sup>13</sup>C]glucose. ITA labeling scheme from [U-<sup>13</sup>C]glutamine (A, red) and [U-<sup>13</sup>C]glucose (B,C) if the *cis*-aconitic decarboxylase (cADC) pathway is active. [U-<sup>13</sup>C]glucose enters glycolysis and results in <sup>13</sup>C<sub>3</sub>-pyruvate, which can enter the TCA cycle as <sup>13</sup>C<sub>2</sub>-acetyl CoA through pyruvate dehydrogenase (PDH), or as <sup>13</sup>C<sub>3</sub>-oxaloacetate through pyruvate carboxylase (PC). The isotopologues of ITA synthesized by this pathway should be predominantly <sup>13</sup>C<sub>1</sub> (PDH flux only, (B, green) or <sup>13</sup>C<sub>4</sub> (both PC and PDH flux, (C, blue). (D) Comparison of isotopologues of ITA, citric acid, and aconitate in VM-M3 cells after incubation with [U-<sup>13</sup>C]-glucose: isotopologues resulting from PDH flux (gray bars) or PC/PDH flux (hatched bars).

the TCA cycle. The NMR data, which show significantly higher <sup>13</sup>C-labeling at the =CH<sub>2</sub> resonance but still an appreciable amount of label at the -CH<sub>2</sub>- resonance in the 1D-gHSQC spectrum, further support this pathway. This route requires the presence of a mammalian homologue of fungal *cis*-aconitic decarboxylase (cADC).<sup>23,24</sup> Other likely routes can be ruled out on the basis of the labeling data (see SI).

The decarboxylation reaction catalyzed by cADC is unique among carboxy-lyases. cADC is the only carboxy-lyase in the ExPASy ENZYME database that catalyzes a decarboxylation resulting in both the reduction of a β-γ unsaturation and the formation of a methyldene group α to the decarboxylation. There are no identifiable mammalian sequence homologues of the *Aspergillus* cADC protein in the NCBI gene database and no structures of the fungal protein to suggest key motifs that could aid in identifying any structural homologues. Hence, we used crude cell extracts to assess *in vitro* synthesis of ITA. Because the RAW 264.7 cells generated a large amount of ITA when stimulated with LPS, we used cell extracts of these to assess *in vitro* synthesis of ITA. Crude RAW 264.7 cell lysates, prepared by Dounce homogenization in a hypotonic buffer, were incubated with 4 mM *cis*-aconitate for 3 h at 37 °C. Metabolites were extracted, lyophilized, and examined by <sup>1</sup>H NMR. There was a 40-fold increase in the intensity of the ITA <sup>1</sup>H resonances compared to control extracts (Figure 5), made either without the addition of *cis*-aconitate or using a boiled cell extract to inactivate any enzyme(s). VM-M3 lysates also generated significant amounts of ITA from *cis*-aconitate (SI, Figure S2). Thus, macrophage-derived cells possess a highly unusual enzymatic activity previously observed only in a few fungi.

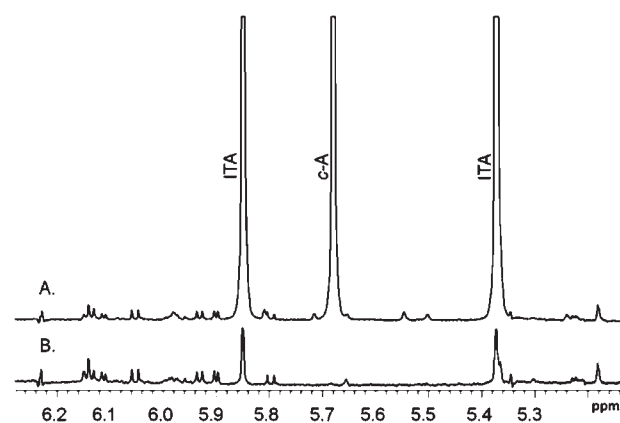


**Figure 5.** *cis*-Aconitate decarboxylase activity in RAW 264.7 crude cell lysates. Comparison of <sup>1</sup>H spectra (600 MHz) of stimulated RAW 264.7 crude extracts incubated at 37 °C in the presence (A) or absence (B) of 4 mM *cis*-aconitate for 3 h. The resonance at 5.67 ppm is residual *cis*-aconitate.

Although ITA can be used to form synthetic polymers, that is unlikely to be its biological function. What is the purpose of the synthesis and excretion of this novel metabolite? ITA has been shown to be a potent inhibitor of isocitrate lyase,<sup>25,26</sup> an enzyme of the glyoxylate cycle found in bacteria, so its secretion could be part of an antibacterial response. However, ITA has also been shown to inhibit phosphofructokinase<sup>27</sup> and, thus, could potentially be involved in regulation of metabolism. It is also possible that ITA acts as a signaling molecule involved in recruitment or regulation of other cells. That ITA levels in cells and culture supernatant significantly increase in response to IFN-γ and LPS points to a potential role in macrophage activation and/or macrophage effector responses. Macrophages are currently known to secrete over 100 substances of various molecular weights that are involved in inflammatory cell activation, proliferation, and effector cell migration.<sup>28</sup> Interestingly, RAW 264.7 conditioned medium has been shown to induce migration and metastasis in colon cancer cells, due at least partially to secretion of chemokines.<sup>29</sup> That the ITA metabolite was first noticed in a metastatic tumor cell line hints that it may also have a role in tumor biology. Observation of this novel metabolite opens up an array of future studies to determine its physiological function, including in the mammalian immune system and in cancer.

## ■ ASSOCIATED CONTENT

**S Supporting Information.** Details of VM-M3 and RAW 264.7 cell culture, murine peritoneal macrophage isolation, preparation of cell extracts, and NMR and LC-MS methods. This material is available free of charge via the Internet at <http://pubs.acs.org>.

## ■ AUTHOR INFORMATION

**Corresponding Author**  
mary.roberts@bc.edu

## ■ ACKNOWLEDGMENT

We thank Roberto Flores and Zeynep Akgoc, Biology Department, Boston College, for assistance with culturing the VM-M3



tumor cells. This work has been supported by the U.S. Department of Energy, Office of Science, Energy Biosciences DE-FG02-91ER20025 (to M.F.R.) and NSF award CBET-0941143 and NIH Challenge Grant 1RC1 CA147961 (to J.D.R.).

## REFERENCES

- (1) Bonnarme, P.; Gillet, B.; Sepulchre, A. M.; Role, C.; Beloeil, J. C.; Ducrocq, C. *J. Bacteriol.* **1995**, *177*, 3573–3578.
- (2) Bentley, R.; Thiessen, C. P. *Science* **1955**, *122*, 330.
- (3) Yu, C.; Cao, Y.; Zou, H.; Xian, M. *Appl. Microbiol. Biotechnol.* **2011**, *89*, 573–583.
- (4) Okabe, M.; Lies, D.; Kanamasa, S. *Appl. Microbiol. Biotechnol.* **2009**, *84*, 597–606.
- (5) Shin, J.; Yang, J.; Jeon, B.; Yoon, Y. J.; Cho, S.; Kang, Y.; Ryu, D. H.; Hwang, G. J. *Proteome Res.* **2011**, *10*, 2238–2247.
- (6) Kvitvang, H. F. N.; Andreassen, T.; Adam, T.; Villas-Boas, S. G.; Bruheim, P. *Anal. Chem.* **2011**, *83*, 2705–2711.
- (7) Wibom, C.; Surowiec, I.; Moren, L.; Bergstrom, P.; Johansson, M.; Antti, H.; Bergenheim, A. T. *J. Proteome Res.* **2010**, *9*, 2909–2919.
- (8) Adler, J.; Wang, S.; Lardy, H. A. *J. Biol. Chem.* **1957**, *229*, 865–879.
- (9) Wang, S.; Adler, J.; Lardy, H. A. *J. Biol. Chem.* **1961**, *236*, 26–30.
- (10) Huysenstruyt, L. C.; Mukherjee, P.; Banerjee, D.; Shelton, L. M.; Seyfried, T. N. *Int. J. Cancer* **2008**, *123*, 73–84.
- (11) Huysenstruyt, L. C.; Shelton, L. M.; Seyfried, T. N. *Int. J. Cancer* **2010**, *126*, 65–72.
- (12) Raschke, W. C.; Baird, S.; Ralph, P.; Nakoinz, I. *Cell* **1978**, *15*, 261–267.
- (13) Cui, Q.; Lewis, I. A.; Hegeman, A. D.; Anderson, M. E.; Li, J.; Schulte, C. F.; Westler, W. M.; Eghbalnia, H. R.; Sussman, M. R.; Markley, J. L. *Nat. Biotechnol.* **2008**, *26*, 162–164.
- (14) Stuckey, D. J.; Anthony, D. C.; Lowe, J. P.; Miller, J.; Palm, W. M.; Styles, P.; Perry, V. H.; Blamire, A. M.; Sibson, N. R. *J. Leukocyte Biol.* **2005**, *78*, 393–400.
- (15) Santini, M. T.; Rainaldi, G.; Ferrante, A.; Romano, R.; Clemente, S.; Motta, A.; De Berardis, B.; Balduzzi, M.; Paoletti, L.; Indovina, P. L. *Chem. Res. Toxicol.* **2004**, *17*, 63–74.
- (16) Shimi, I. R.; Nour El Dein, M. S. *Arch. Microbiol.* **1962**, *44*, 181–188.
- (17) Jakubowska, J.; Metodiewa, D. *Acta Microbiol. Pol. Ser. B: Microbiol. Appl.* **1974**, *6*, 51–61.
- (18) Lu, W.; Clasquin, M. F.; Melamud, E.; Amador-Noguez, D.; Caudy, A. A.; Rabinowitz, J. D. *Anal. Chem.* **2010**, *82*, 3212–3221.
- (19) Bentley, R.; Thiessen, C. P. *J. Biol. Chem.* **1957**, *226*, 703–720.
- (20) Ranzi, B. M.; Ronchetti, F.; Russo, G.; Toma, L. *J. Chem. Soc., Chem. Commun.* **1981**, 785, 1050–1051.
- (21) Merle, M.; Bouzier-Sore, A.-K.; Canioni, P. *J. Neurochem.* **2002**, *82*, 47–57.
- (22) Riazi, R.; Khairallah, M.; Cameron, J. M.; Pencharz, P. B.; Des Rosiers, C.; Robinson, B. H. *Mol. Genet. Metab.* **2009**, *98*, 349–355.
- (23) Dwiarti, L.; Yamane, K.; Yamatani, H.; Kahar, P.; Okabe, M. *J. Biosci. Bioeng.* **2002**, *94*, 29–33.
- (24) Kanamasa, S.; Dwiarti, L.; Okabe, M.; Park, E. Y. *Appl. Microbiol. Biotechnol.* **2008**, *80*, 223–229.
- (25) McFadden, B. A.; Purohit, S. J. *Bacteriol.* **1977**, *131*, 136–144.
- (26) Williams, J. O.; Roche, T. E.; McFadden, B. A. *Biochemistry* **1971**, *10*, 1384–1390.
- (27) Sakai, A.; Kusumoto, A.; Kiso, Y.; Furuya, E. *Nutrition* **2004**, *20*, 997–1002.
- (28) Laskin, D. L.; Pendino, K. J. *Annu. Rev. Pharmacol. Toxicol.* **1995**, *35*, 655–77.
- (29) Green, C. E.; Liu, T.; Montel, V.; Hsiao, G.; Lester, R. D.; Subramaniam, S.; Gonias, L. S.; Klemke, R. L. *PLoS ONE* **2008**, *4*, e6713.